

Experimental Investigation of Radiative and Convective Heat Transfer Coefficients in a Metal Containment Vessel for Small Modular Reactors under Steady-State Conditions

Geunyoung Byeon^a, Beomjin Jeong^a, Namgook Kim^a, Joon-Eon Yang^a, JinHo Song^a, Sung Joong Kim^{a,b*}

^a Department of Nuclear Engineering Hanyang University., 222 Wangsimni-ro, Seongdong-gu Seoul, Korea

^b Institute of Nano Science and Technology, Hanyang University., 222 Wangsimni-ro, Seongdong-gu, Seoul, Korea

*Corresponding author: sungkim@hanyang.ac.kr

***Keywords :** Small modular reactor (SMR), Metal containment vessel (MCV), Heat transfer coefficient (HTC), Radiative heat transfer, Convective heat transfer

1. Introduction

Small modular reactors (SMRs) have garnered global interest due to their enhanced safety characteristics, modular design, and diverse applications, process heat production, and power generation [1-2]. Many SMR designs currently under development incorporate features such as integrated nuclear steam supply systems (NSSS). Among these, a notable structural element in certain SMRs is the metal containment vessel (MCV), which encapsulates the reactor pressure vessel (RPV).

A key design consideration in SMRs is the gap between the RPV and MCV, which plays a crucial role in reactor operation. This gap reduces heat loss during normal operation and serves as a safeguard against pressurization of the MCV caused by steam release from the RPV during reactor transient conditions, such as automatic depressurization valve (ADV) activation.

Various SMR designs employ different gap-filling strategies. These include vacuum conditions or inert gases such as nitrogen and argon. For instance, NuScale VOYGR, developed by NuScale Power in the United States, and the i-SMR, developed by Korea Hydro & Nuclear Power, utilize a vacuum environment (~0.07 bar) within the gap to minimize convective heat transfer and mitigate heat loss [3]. As an alternative, the BWRX-300 by GE-Hitachi employs sub-atmospheric nitrogen within the containment vessel [4], while the ARC-100 by ARC CLEAN TECHNOLOGY utilizes argon gas at slightly above atmospheric pressure [5]. Although the ARC-100 is not a pressurized water reactor (PWR), it adopts a similar approach in terms of containment gas management. The use of inert gases in the containment atmosphere not only influences heat transfer characteristics but also reduces the risk of hydrogen-oxygen combustion during severe accident scenarios [4-5].

Computational fluid dynamics (CFD) analyses have shown that under steady-state conditions, more than 80% of the total heat loss from the RPV to the MCV occurs through radiative heat transfer, regardless of the gap condition [6]. This highlights the dominant role of radiative heat transfer in MCV-based SMR designs and underscores the need for experimental validation of these findings.

To address this, an experimental study was conducted to analyze the temperature distribution under different gap conditions, including vacuum, argon, and nitrogen, based on the normal operating conditions of a small modular reactor. Temperature measurements from various components of the experimental setup were used to calculate the heat transfer rate and to determine the dominant heat transfer mechanism. The results indicated that, except for the case with thermal insulation using Cerakwool, radiative heat transfer was the most dominant mechanism under normal reactor operating conditions for all cases, including vacuum, argon, and nitrogen [7].

Building upon these experimental findings, the present study calculates the heat transfer coefficient using measured temperature data and various correlations. The obtained results are then compared with the previously determined heat transfer rates for different gap conditions, providing further insight into the heat transfer mechanisms governing small modular reactor operation.

2. Methodology

2.1 Experimental apparatus

Fig. 1 presents the experimental setup designed to evaluate total heat losses under steady-state conditions by analyzing heat transfer mechanisms. The core of the chamber contains a cartridge heater, which is surrounded by an SS304 conductor to simulate the RPV. The outer diameter of the experimental chamber was determined based on the pressurizer height of the i-SMR, where the temperature is the highest within the entire reactor region [6]. Since radiative heat transfer becomes more dominant at higher temperatures, this region was selected to simulate its effects. To minimize axial heat losses and focus on radial heat transfer, Cerakwool insulation was applied to the upper and lower flanges. Table I summarizes the geometric specifications of the test section components.

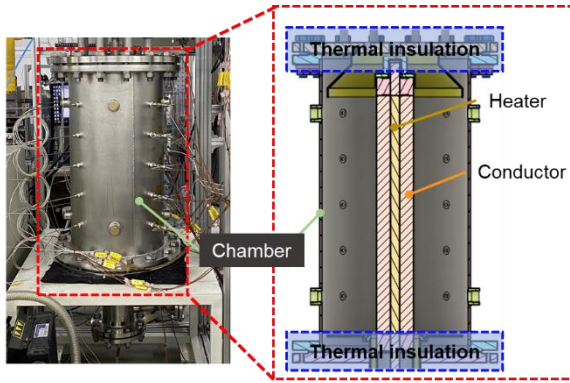


Fig. 1. Cross-section of a conjugate heat transfer experimental apparatus (before insulation) [7]

Table I: Geometric specifications of the test section components

Component	Specification
Cartridge heater	Diameter: 0.0254m Length: 0.85m
SS304 conductor	Outer diameter: 0.1016m
Experimental chamber	Outer diameter: 0.406m Wall thickness: 0.006m Height: 0.85m
Insulation material	Ceramic fiber (Cerakwool)

2.2 Measurement points

Fig. 2 illustrates the locations of pressure and temperature measurement points within the experimental setup. Pressure is monitored using two pressure transmitters, positioned at the top and bottom of the chamber. Temperature measurements are conducted using multiple K-type thermocouples strategically placed at various locations. Specifically, the heater section contains three K-type thermocouples at five different heights, positioned at varying depths. In the region between the conductor and chamber wall, which represents the SMR's gap, two K-type thermocouples are installed at each of the five heights. Additionally, the chamber wall, which simulates the SMR's MCV, is instrumented with three T-type thermocouples at each of the five heights. T-type thermocouples were selected for the chamber wall due to their lower measurement error compared to K-type thermocouples within the target temperature range. To assess the ambient air temperature, five resistance temperature detectors (RTDs) are positioned outside the chamber wall, one at each height.

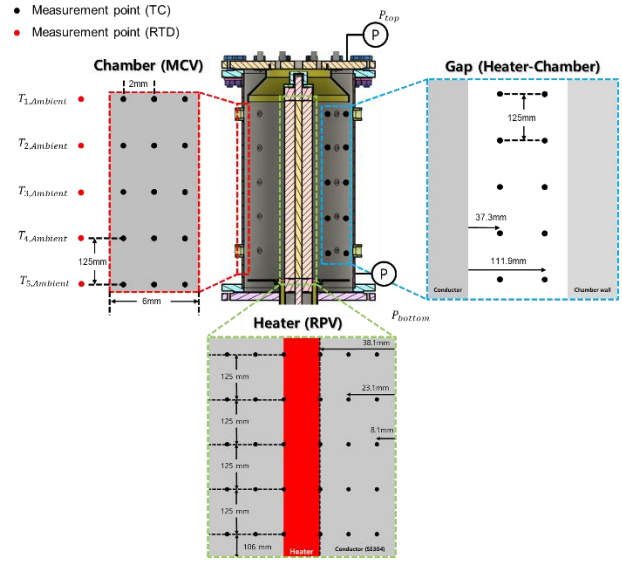


Fig. 2. Measurement points of the experimental apparatus (Heater, Gap, Chamber wall) [7]

2.3 Test matrix & Experimental procedure

The experiment was performed under steady-state conditions to evaluate heat loss from the MCV during normal reactor operation. Based on previous CFD studies, the surface temperature of the heater conductor was maintained at 320°C at the mid-height of the heater for all test cases [6]. Unlike certain currently developed SMR designs, this study assumed that the exterior of the MCV was air-cooled. For the vacuum condition, a pressure of 0.07 bar was established, following the conditions used in NuScale's VOYGR [3]. Under this scenario, heat loss was considered to occur exclusively through conduction and radiative heat transfer. For the nitrogen and argon cases, the selection was based on their use as containment fill gases in BWRX-300 and ARC-100, respectively. Lastly, although carbon dioxide (CO₂) is not currently utilized as a containment fill gas in existing reactor designs, it was included in this study due to its radiative absorption properties [8].

Regarding the experimental procedure, for gas-filled conditions, gas was initially injected at room temperature, and to minimize the residual air fraction, the gas injection and vacuum evacuation process was repeated three times. The cartridge heater was then powered using a DC power supply. Once the surface temperature of the heater conductor reached 320°C and steady-state conditions were established, the experiment was terminated. Steady state was defined as the condition in which the surface temperature of the heater conductor remained within $\pm 0.2^\circ\text{C}$ for 15 minutes, and the temperatures of all components stabilized within 0.05°C.

Direct temperature measurement of the heater conductor surface using thermocouples was challenging due to attachment difficulties. Instead, the heat transfer rate was determined based on radial temperature measurements, and the surface temperature of the heater

conductor was back-calculated accordingly. The test matrix summarizing the experimental conditions is presented in Table II.

Table II: Test matrix

Heater Surface Temperature	~ 320 °C
Ambient Temperature	~ 20 °C
Initial Pressure	0.07 bar (Vacuum)
	1.00 bar (Nitrogen, Argon, CO ₂)
Gap condition	Vacuum
	Nitrogen
	Argon
	CO ₂

3. Result and Discussion

This section presents the experimental results for each gap condition and includes the corresponding analytical findings based on these results.

3.1 Required Heater Power

Table III presents the required heater power to maintain the surface temperature of the heater conductor at 320°C. A lower required power indicates reduced heat loss to the surroundings, allowing for an assessment of efficiency in the order of vacuum, argon, nitrogen, and carbon dioxide in terms of heat loss. Notably, the heat loss in the vacuum gap condition was significantly lower compared to the gas-filled gap conditions. This is attributed to the minimal contribution of natural convection to heat loss in the vacuum gap condition, as conduction and radiative heat transfer dominate in the absence of gas. As a result, the overall heat loss is significantly lower compared to gas-filled gap conditions.

Table III: Power applied via DC supply for each case

	Voltage (V)	Current (A)	Power (W)
Vacuum	59.6	5.72	340.912
Argon	74.4	7.09	527.496
Nitrogen	79.5	7.58	602.610
CO ₂	83.0	7.91	656.530

3.2 Temperature distribution

Fig. 3 and Fig. 4 present the temperature distribution as a function of distance for each case and the temperature distribution in each region, respectively. In selecting the test matrix, steady-state conditions were defined such that the calculated surface temperature of the heater conductor at the mid-height remained within 320°C ± 0.2°C at five axial measurement points.

Therefore, temperature measurements in the radial direction at the mid-height were analyzed.

The regional temperature distribution indicates that, for gas-filled conditions, higher DC power input generally results in elevated temperatures across all regions. In the case of carbon dioxide, its strong radiative absorption properties lead to increased heat absorption, which in turn enhances heat loss through natural convection. As a result, the overall heat loss in the CO₂ - filled condition is higher compared to other gas-filled cases.

Conversely, in the case of argon, its relatively low thermal conductivity induces an insulating effect near the heater conductor and chamber wall [9]. This results in lower temperatures across all components compared to other gas-filled conditions.

For the vacuum case, as previously mentioned, natural convection does not play a dominant role in heat loss mechanisms. Consequently, the overall heat loss is significantly reduced. Additionally, a steep temperature gradient is observed in the gap region. This is attributed to the near absence of fluid motion within the test section, leading to a high temperature near the heater conductor, while the chamber wall remains relatively cooler due to heat loss occurring solely through radiation and conduction. This insulating effect reduces the required heater power, and apart from the area near the heater conductor, the overall temperatures in the vacuum condition remain lower than those in gas-filled conditions.

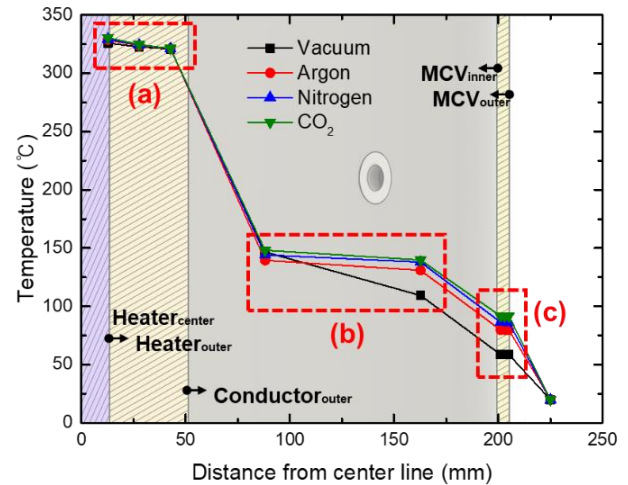


Fig. 3. Temperature distribution of each gap condition based on distance from the center line of test section (for middle height region)

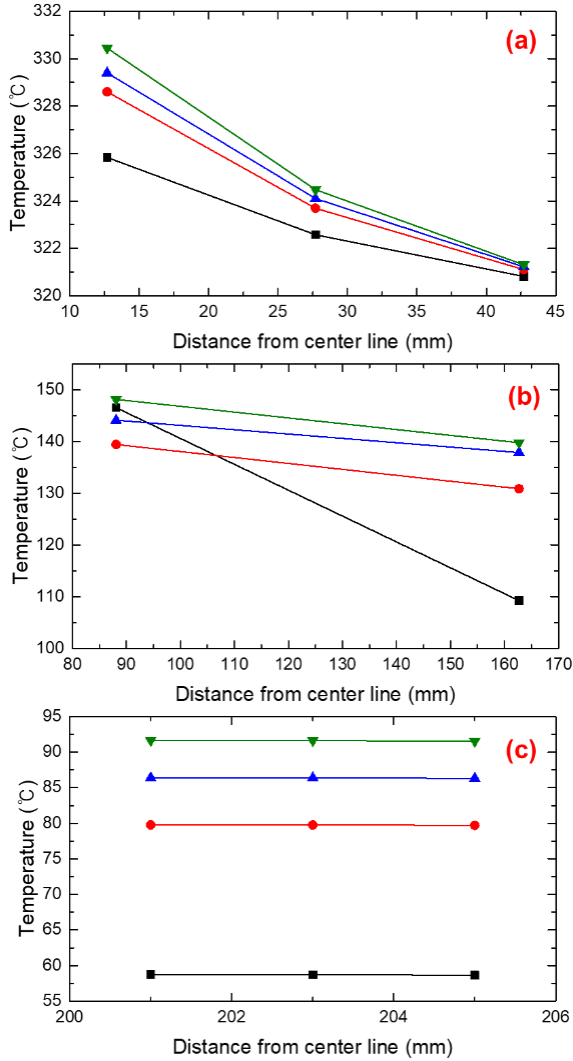


Fig. 4. Temperature distribution of each gap conditions based on distance from the center line of test section (a): Heater conductor, (b): Gap region, (c): Chamber wall

3.3 Heat transfer rate (HTC) calculation

The natural convection heat transfer coefficient was derived from empirical correlations, whereas the radiative heat transfer coefficient was determined based on measured temperature and effective emissivity. Considering the cylindrical configuration of the enclosure, key dimensionless numbers, including the Rayleigh number (Ra) and Prandtl number (Pr), were utilized to characterize natural convection behavior. The Rayleigh number within the gap was computed using Eq. (1), with the corresponding results presented in Table IV.

The values reported in Table IV represent the averaged surface temperatures of all components, obtained by evaluating data across multiple axial measurement points. The thermophysical properties of the gap-filling gases were assessed at the bulk temperature, while pressure readings were acquired from a pressure transmitter. Thermal diffusivity and kinematic viscosity values were referenced from NIST REFPROP [9]. The thermal

expansion coefficient (β) was estimated based on the ideal gas assumption, given by $\beta = 1/T$, where T denotes the absolute temperature.

$$Ra = \frac{g\beta(r_{CH,i} - r_{HC,o})^3(T_{HC,o} - T_{CH,i})}{\nu\alpha} \quad (1)$$

Table IV: Surface temperatures and Rayleigh number for the heater conductor (HC) and chamber (CH) inner surface under various gap candidates

Candidate	Surface temperature of HC	Inner surface temperature of the CH	Rayleigh number (Ra)
Vacuum	311.480°C	59.171°C	3.822×10^5
Argon	311.312°C	79.951°C	1.359×10^8
Nitrogen	311.140°C	86.776°C	1.120×10^8
CO ₂	311.404°C	90.381°C	3.462×10^8

To evaluate the heat transfer characteristics, the Nusselt number (Nu) was calculated using empirical correlations established by Davis et al. [10] and Nagendra et al. [11], which describe convective heat transfer within cylindrical enclosures. The correlation formulated by Davis et al. was applied under the condition that $Ra > 2 \times 10^5$, whereas the more general correlation from Nagendra et al. was employed for all cases. Table V provides a summary of the correlations utilized to determine the natural convection HTC and radiative HTC. The emissivity values of the heater conductor surface and the chamber inner wall were obtained from prior studies [12-13].

Table V: Correlations used for natural convective HTC and radiative HTC in this study

Davis et al. [10]
$Nu = 0.286 \cdot Ra^{0.258} \cdot Pr^{0.006} \cdot H^{-0.238} \cdot K^{0.442}$
where
$R = r_{CH,i} - r_{HC,o}; H = \frac{L}{R}; K = \frac{r_{CH,i}}{r_{HC,o}}$
Nagendra et al. [11]
$Nu = 0.48 \cdot Ra \cdot \left[6830 \cdot \left(\frac{L}{r_{CH,i}} \right)^4 \cdot \frac{r_{HC,o}}{L} + Ra^{\frac{3}{4}} \right]^{-1}$
$\frac{L}{r_{HC,o}} Ra^{-\frac{1}{4}} < 0.1$
$Nu = 1.19 \cdot Ra \cdot \left[16900 \cdot \left(\frac{L}{r_{CH,i}} \right)^4 \cdot \frac{r_{HC,o}}{L} + Ra^{0.84} \cdot \left(\frac{r_{HC,o}}{L} \right)^{0.36} \right]^{-1}$
$0.1 \leq \frac{L}{r_{HC,o}} Ra^{-\frac{1}{4}} \leq 0.738$
Radiative HTC
$h_{rad} = \sigma \cdot \varepsilon_{eff} \cdot (T_{HC,o}^2 + T_{CW,i}^2) \cdot (T_{HC,o} + T_{CW,i})$
where
$\varepsilon_{eff} = \left[\frac{1 - \varepsilon_{HC,o}}{\varepsilon_{HC,o}} + \frac{1}{F_{HC-CW}} + \left(\frac{1 - \varepsilon_{HC,i}}{\varepsilon_{HC,i}} \right) \cdot \frac{r_{HC,o}}{r_{HC,i}} \right]^{-1}$

Using these correlations, the HTC values for natural convection and radiation were calculated, as presented in Table VI. Since radiative and convective heat transfer

occur in parallel, the HTC values were derived based on temperature measurements.

Table VI: HTCs for natural convection and radiation under various gap candidates using the Davis et al. and Nagendra et al. correlation.

Candidate	HTC for radiation	HTC for natural convection (Davis et al.)	HTC for natural convection (Nagendra et al.)
Vacuum	3.62 W/m ² K	0.53 W/m ² K	0.13 W/m ² K
Argon	3.81 W/m ² K	1.63 W/m ² K	1.74 W/m ² K
Nitrogen	3.88 W/m ² K	2.28 W/m ² K	2.43 W/m ² K
CO ₂	3.92 W/m ² K	2.37 W/m ² K	2.57 W/m ² K

Table VI shows that, except for the vacuum gap case, the HTC values obtained from the two correlations were in close agreement. Additionally, a higher combined HTC for radiation and natural convection indicates a greater overall heat loss to the surroundings. In this regard, the trend of HTC analysis aligns with the trend observed in DC power input. Lastly, a comparison of the HTC values reveals that the radiative HTC is greater than the natural convective HTC. This finding is consistent with previous research [7], which demonstrated that in SMRs with narrow gaps, radiative heat transfer dominates among the heat transfer mechanisms contributing to heat loss.

4. Conclusions

This study experimentally investigated the heat transfer characteristics in the gap between the RPV and the MCV under various gap conditions, including vacuum, argon, nitrogen, and carbon dioxide. The results provide valuable insights into the dominant heat transfer mechanisms governing heat loss in SMRs utilizing an MCV-based containment structure.

The experimental results confirmed that radiative heat transfer plays a dominant role in heat loss for all gap conditions, which aligns with previous CFD analyses indicating that over 80% of the total heat loss occurs through radiation. Furthermore, HTCs for natural convection and radiation were derived using empirical correlations from Davis et al. and Nagendra et al.

Among the tested conditions, the vacuum gap demonstrated the lowest heat loss due to the absence of natural convection, as heat transfer was primarily governed by radiation and conduction. The steep temperature gradient observed in the gap region further supports the insulating effect of the vacuum condition, which significantly reduces the required heater power. In contrast, gas-filled conditions exhibited higher heat loss, with carbon dioxide showing the highest due to its radiative absorption properties. Argon, with its low thermal conductivity, exhibited an insulating effect near

the heater conductor and chamber wall, resulting in lower temperatures compared to other gases.

However, it should be noted that the experimental setup was designed based on the assumption that radiative heat transfer is the dominant heat loss mechanism, and thus, it does not account for the scaling of convection effects. Moreover, the experimental apparatus used in this study was constructed at a reduced scale compared to an actual SMR. Therefore, heat transfer phenomena observed in scaled-down experiments may differ from those in real reactor conditions. In particular, the relative importance of heat transfer mechanisms (radiation versus convection) in a scaled-down setup might differ significantly from the conditions expected in a full-scale reactor.

The findings of this study reinforce the critical role of radiative heat transfer in MCV-based SMRs and highlight the impact of gap conditions on thermal performance. These results can serve as a reference for optimizing thermal management in the next-generation SMR designs.

The findings of this study reinforce the critical role of radiative heat transfer in MCV-based SMRs and highlight the impact of gap conditions on thermal performance. These results can serve as a reference for optimizing thermal management in the next-generation SMR designs.

5. Acknowledgement

This work was supported by the Innovative Small Modular Reactor Development Agency grant funded by the Korea Government (MSIT) (No. RS-2024-00404240). Additionally, this work was supported by the Innovative Small Modular Reactor Development Agency grant funded by the Korea Government (MSIT) (No. RS-2023-00259516).

REFERENCES

- [1] M.D. Carelli et al., "Economic features of integral, modular, small-to-medium size reactors," *Progress in Nuclear Energy*, 52 (4), pp. 403-414 (2010).
- [2] D.T. Ingersoll et al., "NuScale small modular reactor for Co-generation of electricity and water," *Desalination*, 340, pp. 84-93 (2014).
- [3] Reyes Jr, José N. "NuScale plant safety in response to extreme events." *Nuclear Technology* 178.2 (2012): 153-163
- [4] Energy, GE Hitachi Nuclear. "BWRX-300 General Description." (2023)
- [5] ARC CLEAN TECHNOLOGY
- [6] Lee, Geon Hyeong, et al. "Analysis of heat-loss mechanisms with various gases associated with the surface emissivity of a metal containment vessel in a water-cooled small modular reactor." *Nuclear Engineering and Technology* (2024).
- [7] Byeon, Geunyoung, JinHo Song, and Sung Joong Kim. "Experimental Study on the Heat Loss Mechanism in a Metal Containment Vessel under Various Gap Conditions during

- Normal Operation of a Small Modular Reactor" Transactions of the Korean Nuclear Society Autumn meeting, pp.1-5 (2024)
- [8] El-Shobaky, G. A., Th El-Nabarawy, and A. M. Dessouki. "Adsorption properties of gamma-irradiated carbons." *International Journal of Radiation Applications and Instrumentation. Part C. Radiation Physics and Chemistry* 30.3 (1987): 161-163.
- [9] Lemmon, Eric W., et al. "REFPROP documentation." *Release 10* (2018): 135.
- [10] Thomas, R. W., and Graham de Vahl Davis. "Natural convection in annular and rectangular cavities a numerical study." *International Heat Transfer Conference Digital Library*. Begel House Inc., 1970.
- [11] Nagendra, H. R., M. A. Tirunarayanan, and A. Ramachandran. "Free convection heat transfer in vertical annuli." *Chemical Engineering Science* 25.4 (1970): 605-610.
- [12] Pelenovich, Vasily O., et al. "Oxidized textured stainless steel surface with passivation layer as a high temperature selective solar absorber." *Ceramics International* 50.22 (2024): 47215-47222.
- [13] Winter, Michael, et al. "Spectral, directional emittance of stainless steel at elevated temperatures." *Journal of Thermophysics and Heat Transfer* 33.2 (2019): 495-507.